Acta Cryst. (1978). B**34**, 701–705

Refinement of an *R* Phase, $Mn_{85\cdot5}Si_{14\cdot5}$*

BY CLARA BRINK SHOEMAKER AND DAVID P. SHOEMAKER

Department of Chemistry, Oregon State University, Corvallis, Oregon 97331, *USA*

(*Received* 18 *July* 1977; *accepted* 9 *September* 1977)

The structure of the *R* phase has been refined by full-matrix least squares with diffractometer data from a single-crystal fragment of $Mn_{85\cdot5}Si_{14\cdot5}$. The rhombohedral lattice constants are: a = 8·959 (3) Å, α = 74·70 (3)°, the hexagonal lattice constants: a = 10·871 (5), c = 19·180 (9) Å. The space group is $R\bar{3}$ (C_{3i}^2), 53 atoms per rhombohedral cell. The final $R(F)$ for the refinement with anisotropic thermal parameters is 0·052 for the 593 reflections with $I > 2\sigma$ included in the refinement, or 0·151 for all 1302 reflections. This refinement confirms that the *R* phase has an ideally tetrahedrally close-packed structure, and that it therefore deviates significantly in structure from the ε phase ($Mg_{23}Al_{30}$) determined by S. Samson & E. K. Gordon [*Acta Cryst.* (1968), B**24**, 1004–1013]. The positions with CN > 12 are occupied by Mn, the positions with CN = 12 by mixtures of Mn and Si. The largest percentages of Si occur in the icosahedral positions on the threefold axes. Si–Si contacts do not occur, except possibly between sites that are occupied by mixtures of Mn and Si.

Introduction

This work represents a continuation of our study of the role of Si in tetrahedrally close-packed (t.c.p.) transition-metal alloys. We have previously reported the structures of the ν or N phase ($Mn_{81\cdot5}Si_{18\cdot5}$; Shoemaker & Shoemaker, 1971) which is ideally t.c.p., the *K* phase ($Mn_{77}Fe_4Si_{19}$; Shoemaker & Shoemaker, 1977) which also is ideally t.c.p., and the *D* phase (Mn_5Si_2; Shoemaker & Shoemaker, 1976) which is mainly t.c.p. but has some irregular coordinations. An *R* phase in the Mn–Si system was discovered by Kuzma & Hladyshevskii (1964) and confirmed by Bardos & Beck (1965). The structure of the *R* phase was first determined with photographic data, for the alloy $Mo_{30\cdot4}Co_{51\cdot3}Cr_{18\cdot3}$ (Komura, Sly & Shoemaker, 1960). The *R* factor obtained in that determination for 521 observed reflections was 0·096. Subsequently, Samson & Gordon (1968) determined the structure of ε-$Mg_{23}Al_{30}$ with diffractometer data and refined this structure to R = 0·021 for 1469 measured reflections. The structure of this latter phase turned out to be very similar to that of the *R* phase but with some distinct differences in coordination resulting from atomic parameter differences a few of which are as large as 0·75 Å. The *R* phase is ideally t.c.p., but in the ε phase some non-tetrahedral interstices (including distorted octahedra) also occur. Since the original *R*-phase structure determination was done only with photographic data, one of the objectives of the refinement of $Mn_{85\cdot5}Si_{14\cdot5}$ with diffractometer data was to confirm with greater certainty that the *R* phase and the ε phase are indeed distinctly different in structure.

Experimental

The specimen used by us was prepared by Bardos & Beck (1965) by induction heating of the appropriate mixture of the two component elements in a helium atmosphere followed by 7 d of annealing at 800°C. At that temperature, according to the phase diagram given by Bardos & Beck, the stability range is about 13·8 to 15·4 at.% Si. At about 870°C and 15·2 at.% Si the phase decomposes into a more Si-rich phase (the ν

Table 1. *Crystal data for the R phase,* $Mn_{85\cdot5}Si_{14\cdot5}$

FW/atom		51·04	Space group	$R\bar{3}$ (C_{3i}^2)
Rhombohedral	a (Å)	8·959 (3)	Atoms/rhombohedral cell	53
	α (°)	74·70 (3)	D_x (g cm^{-3})	6·86
	V (Å^3)	654·3 (4)	F(000)	1245
Hexagonal	a (Å)	10·871 (5)	μ(Mo $K\alpha$)(cm^{-1})	222
	c (Å)	19·180 (9)		

---

* Research supported by National Science Foundation Grant DMR76-80559.

phase) and a less Si-rich phase (having the β-Mn atomic arrangement). The specimen as received by us was crushed in a mortar and a fragment suitable for diffraction work was identified by microscopic examination.

The crystal data for the *R* phase, $\mathrm{Mn_{85\cdot5}Si_{14\cdot5}}$ are given in Table 1. Intensity data for a crystal fragment in arbitrary orientation were collected with Mo $K\alpha$ radiation on an automated Syntex $P\bar{1}$ diffractometer equipped with a graphite monochromator. A θ–2θ scan was used, the scan speed was 1° $\mathrm{min^{-1}}$, the 2θ range was 2·0° plus the $\alpha_1\alpha_2$ angular separation. Background readings were made at the beginning and the end of each scan range; the ratio of background time to scan time was 1 to 2. About 4200 reflections, of which 1300 were independent, were measured in a half sphere of reciprocal space out to $2\theta = 60°$. The crystal fragment was irregularly shaped with dimensions varying between 0·044 and 0·076 mm. Each independent reflection was measured at three or four different positions in reciprocal space and an absorption correction was applied to the averaged intensities, assuming spherical shape with $\mu r = 0\cdot70$, corresponding to a range in the transmission factors of 4%. A secondary extinction correction was not applied. The real and imaginary parts of the anomalous dispersion were taken into account (Cromer & Liberman, 1970).

Table 2. *Agreement factors for the least-squares refinements of the R phase,* $\mathrm{Mn_{85\cdot5}Si_{14\cdot5}}$

NO	Thermal parameters	NV	$R(F)$	$R_w(F)$	S^*
1302	Isotropic	44	0·151	0·079	0·851
593, $I > 2\sigma$	Isotropic	44	0·056	0·064	1·035
1302	Anisotropic	87	0·149	0·075	0·822
593, $I > 2\sigma$	Anisotropic	87	0·052	0·059	0·997

$^*S = \{\Sigma[W(F_c - F_o)^2]/(\mathrm{NO} - \mathrm{NV})\}^{1/2}$.

Structure refinement

The data reduction and initial structure factor calculations were done on the Oregon State University CDC 3300 and CYBER 73 computers with local versions of the programs *STUDIT*, *INCOR* (Zalkin) and *LSLONG* (based on Zalkin's modification of the Gantzel–Sparks–Trueblood refinement program). The scattering factors for the neutral atoms were taken from *International Tables for X-ray Crystallography* (1962). The weights were based on the standard errors in the intensities I_o as estimated with the equation $\sigma(I_o) = [C + Bt^2 + (0\cdot05C)^2 + (t0\cdot05B)^2]^{1/2}$ (C is the integrated count, B is the total background count, $t = 2$ is the ratio of the scan time over the background time). The intensities of the equivalent reflections were averaged and so were the σ's, except that when the ratio of the scatter (*i.e.* range) to the average σ in the set of equivalent reflections was larger than 1, the average σ was replaced by the scatter. The refinements were done on the Lawrence Berkeley Laboratory CDC 7600 computer with the *NUCLS* program contained in Zalkin's XRAY 76 program system, from a remote terminal through the courtesy of the Pacific Northwest Laboratory of the Environmental Protection Agency, Corvallis.

Refinement

The agreement factors obtained in the least-squares refinements are listed in Table 2. Since more than half of the independent reflections have intensities smaller than 2σ, the parameters obtained on anisotropic refinement with the 593 intensities larger than 2σ are considered to be the final ones. These final parameters, listed in Table 3, are in almost all cases closer to those derived previously for *R* (Mo–Co–Cr) than they are to those for ε (Mg–Al). Five refinement cycles starting with the positional parameters of the ε phase as initial parameters resulted in parameter shifts of up to 58σ, all

Table 3. *Atomic parameters for the R phase,* $\mathrm{Mn_{85\cdot5}Si_{14\cdot5}}$

Positional parameters are from anisotropic refinement; *B* values are from isotropic refinement ($I > 2\sigma$ in each case). Names and CN for the corresponding atoms in the ε phase are also given.

CN	Atom	x_{rh}	y_{rh}	z_{rh}	B (Å^2)	f_0	% Mn	ε phase Atom	ε phase CN
12	*A*(1)	½	½	½	0·20 (31)	15·1 (1·2)	10 (10)	Mg(1)	14
12	*A*(2)	0·30574 (42)	0·30574	0·30574	0·53 (20)	17·0 (0·8)	27 (8)	Mg(2)	13
12	*A*(3)	0·16213 (40)	0·08819 (41)	0·75392 (43)	0·71 (10)	21·5 (0·5)	67 (5)	Al(7)	12
12	*A*(4)	0·15384 (42)	0·32940 (41)	0·82067 (42)	0·77 (9)	22·0 (0·5)	72 (4)	Al(8)	12
12	*A*(5)	0·21413 (37)	0·31450 (36)	0·05517 (36)	0·57 (9)	22·9 (0·5)	81 (4)	Al(9)	12
12	*A*(6)	0·48520 (47)	0·23740 (40)	0·07054 (45)	0·52 (8)	21·8 (0·4)	71 (4)	Al(10)	12
14	*B*(1)	0·57258 (36)	0·35249 (38)	0·26965 (35)	0·77 (5)		100	Al(11)	11
14	*B*(2)	0·57657 (39)	0·62002 (39)	0·20087 (37)	0·88 (5)		100	Mg(6)	14
15	*C*(1)	0·35259 (40)	0·53886 (38)	0·05883 (43)	0·81 (5)		100	Mg(5)	14
16	*D*(1)	0·07392 (32)	0·07392	0·07392	0·88 (8)		100	Mg(3)	16
16	*D*(2)	0·39080 (41)	0·07830 (38)	0·89834 (41)	0·85 (5)		100	Mg(4)	16

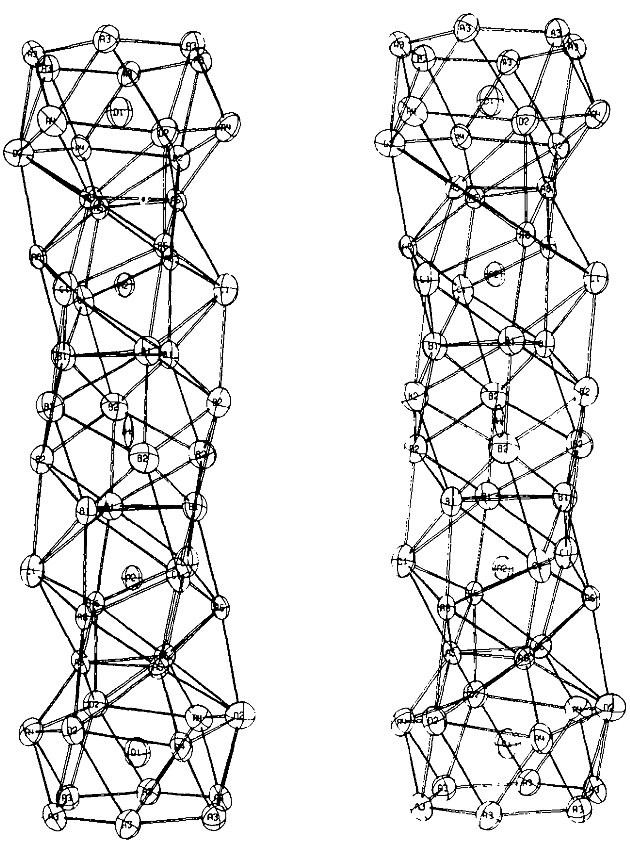

Fig. 1. Stereoscopic view produced by *ORTEP* of the polyhedra along the threefold axis in R-$Mn_{85\cdot5}Si_{14\cdot5}$. The thermal ellipsoids (and also those in Fig. 2) are drawn for 99% probability. Atom $A(1)$ (at a center of symmetry) and atoms $A(2)$ are at the centers of icosahedra. They are not near neighbors, as they are in the ε phase. An additional $D(1)$ atom outside the six-membered ring formed by the $A(3)$ atoms completes the CN 16 polyhedron around $D(1)$.

leading to values close to the R (Mo–Co–Cr) parameters. The R factor in these cycles decreased from 0·408 to 0·131 ($I > 2\sigma$).*

Description of the structure

The largest differences in positional parameters between the R phase and the ε phase occur for atom $A(2)$ corresponding to Mg(2) and atom $B(1)$ corresponding to Al(11) and amount to 0·75 and 0·6 Å. Fig. 1 is a stereoscopic picture of the surroundings of the threefold axis in the R phase, which may be compared with Fig. 2 of Samson & Gordon (1968) which gives the corresponding arrangement in the ε phase. For the Si atoms, $A(1)$ and $A(2)$, the shapes of the ellipsoids are not to be regarded as significantly different from spheres because of the large relative uncertainties in the anisotropic parameters. In the R phase the sequence of polyhedra along the threefold axis is: CN 16 [$D(1)$], CN 12 [$A(2)$], CN 12 [$A(1)$], CN 12 [$A(2)$], CN 16 [$D(1)$]. In the ε phase the central icosahedron has been broadened, mainly by moving Al(11) [$B(1)$] away from the threefold axis, thus allowing the Mg(2) [$A(2)$] atoms at the centers of the icosahedra above and below to move within near-neighbor distance of atom Mg(1) [$A(1)$] centering the central original icosahedron. As a result, Mg(1) has CN 14 with atoms arranged at the corners of a distorted hexagonal prism with two Mg(6) [$B(2)$] atoms at the extended poles. Mg(2) has one Mg(1) as an additional neighbor and has thus CN 13. Note that the icosahedra along the threefold axis in the R phase are enlarged in the ε phase, so that they may be occupied by the larger Mg atoms. Fig. 2 illustrates the arrangement observed in the R phase (*cf.* Fig. 3 of Samson & Gordon, 1968). $A(1)$ and $A(2)$ in the R phase are not near neighbors, as they are in the ε phase. Atom Mg(5) [$C(1)$] has lost one of the neighboring Al(11) [$B(1)$] atoms and has now CN 14 (distorted hexagonal antiprism + 2). $B(1)$ which has CN 14 in the R phase is occupied by the smaller atom in the ε phase: Al(11) with CN reduced to 11. The coordinations for the remaining atoms are the same in the two phases with the Al atoms occupying the icosahedral sites and the Mg atoms the positions with CN larger than 12. Thus, although the R phase and the ε phase are in a sense isotypic there are significant differences in the atomic parameters which correlate with the ordering of the larger and smaller atoms in ε-$Mg_{23}Al_{30}$. The ε phase is not t.c.p.: there are, for example, six distorted octahedral interstices with atom Mg(1) as a common apex.

We have demonstrated (Shoemaker & Shoemaker, 1963) that for ideally t.c.p. structures one can derive from the observed interatomic distances a set of five- and six-coordinated radii (minor and major radii) for each coordination type. For the Mo–Co–Cr R phase this has been described by Komura *et al.* (1960). A major bond is about 0·4 Å shorter than a minor bond between the same pair of atoms. Table 4 shows that this applies to the observed interatomic distances in R-$Mn_{85\cdot5}Si_{14\cdot5}$. A prominent feature of t.c.p. structures is the 'major network' formed by the six-coordinated or major bonds. In the R phase the major bonds form one three-dimensional network which is shown stereoscopically in Fig. 3.

In the ε phase the distances do not lead to a consistent set of minor and major radii for each coordination type. One can trace a three-dimensional network of six-coordinated bonds as for the R phase, but there are distortions which cause interconnections involving atoms $C(1)$, $B(1)$ and $B(2)$ to be missing.

---

* A list of structure factors, based on the final parameters listed in Table 3, has been deposited with the British Library Lending Division as Supplementary Publication No. SUP 33036 (7 pp.). Copies may be obtained through The Executive Secretary, International Union of Crystallography, 13 White Friars, Chester CH1 1NZ, England.

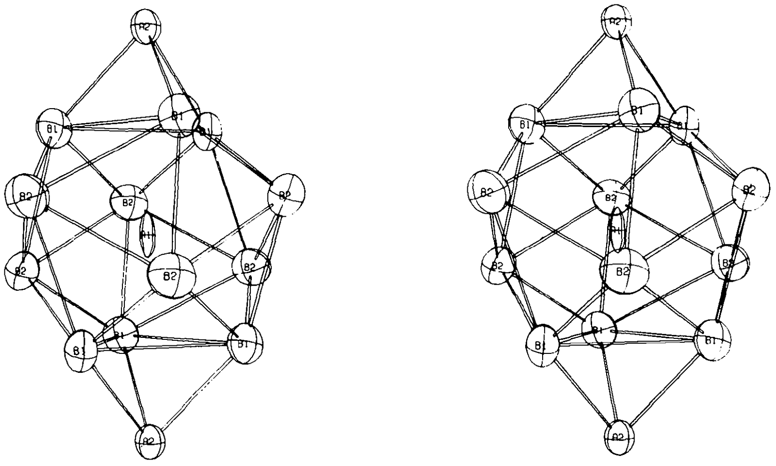

Fig. 2. Stereoscopic view produced by *ORTEP* of the center part of Fig. 1.

Table 4. *Interatomic distances for* $\mathrm{Mn}_{85\cdot5}\mathrm{Si}_{14\cdot5}$

Asterisks indicate major bonds. MS represents a mixture of Mn and Si.

		A(1)	*A*(2)	*A*(3)	*A*(4)	*A*(5)	*A*(6)	*B*(1)	*B*(2)	*C*(1)	*D*(1)	*D*(2)
	% Mn	10	27	67	72	81	71	100	100	100	100	100
	CN	12	12	12	12	12	12	14	14	15	16	16
A(1) Si	12							2·590	2·590			
A(2) MS	12					2·562	2·403	2·459		2·639		
A(3) MS	12			2·365 2×	2·368 2·429		2·359	2·607		2·697 2·749	2·743 3× 2·771 3×	2·669 2·755
A(4) MS	12			2·368 2·429		2·266	2·325	2·536	2·511 2·522	2·812	2·858 3×	2·736 2·771 2·844
A(5) MS	12		2·562 3×		2·266	2·462 2×	2·374 2·415		2·593	2·637	2·716 3×	2·642 2·694 2·754
A(6) MS	12		2·403 3×	2·359	2·325	2·374 2·415		2·644	2·559	2·626 2·634 2·698		2·720 2·759
B(1) Mn	14	2·590 6×	2·459 3×	2·607	2·536		2·644	2·948 2×	2·319* 2·752 2·816	2·614* 2·802 2·967		3·025
B(2) Mn	14	2·590 6×			2·511 2·522	2·593	2·559	2·319* 2·752 2·816	2·828 2×	2·887 2·963		2·682* 3·183
C(1) Mn	15		2·639 3×	2·697 2·749	2·812	2·637	2·626 2·634 2·698	2·614* 2·802 2·967	2·887 2·963	2·553*		2·695*
D(1) Mn	16			2·743 2·771	2·858	2·716					2·836*	2·864*
D(2) Mn	16			2·669 2·755	2·736 2·771 2·844	2·642 2·694 2·754	2·720 2·759	3·025	2·682* 3·183	2·695*	2·864* 3×	2·863*

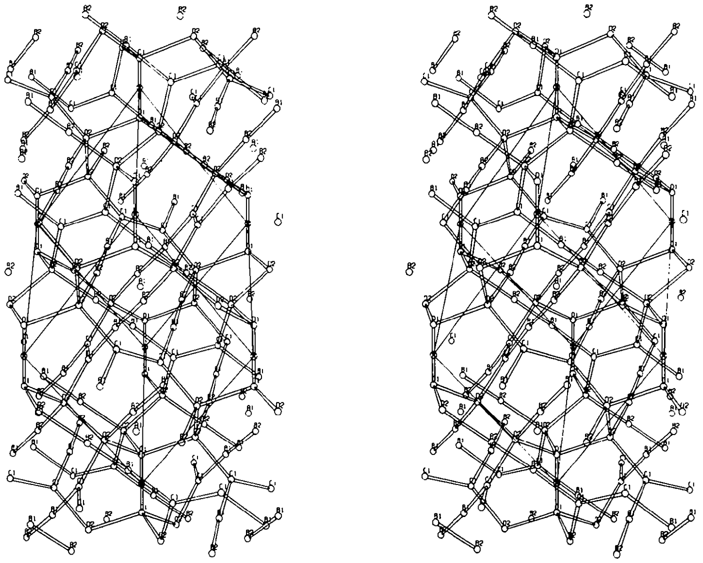

Fig. 3. Stereoscopic view produced by *ORTEP* of the three-dimensional 'major network' of six-coordinated bonds in R-$Mn_{85\cdot5}Si_{14\cdot5}$. The rhombohedral unit cell has been drawn in. In the ε phase there are distortions which destroy links $C(1)$–$C(1)$, $C(1)$–$B(1)$ and $B(1)$–$B(2)$.

Another example of essentially isotypic intermetallic compounds which have significant differences in parameters is represented by the structures of Sm_5Ge_4 (Smith, Johnson & Tharp, 1967), Gd_5Si_4 (Iglesias & Steinfink, 1972), and Pu_5Rh_4 (Cromer, 1977).

Ordering of the atoms

In the final least-squares refinement cycles the occupancies of the CN 12 sites were varied. The sites with CN > 12 were assumed to be solely occupied by Mn atoms because of the small range in the temperature factors for these sites based on this assumption. It was found (Table 3) that site $A(1)$ is, within one standard deviation in the occupancy parameter, occupied by Si only. Site $A(2)$ contains a small amount of Mn ($3\cdot5\sigma$) and the other CN 12 sites contain larger amounts of Mn with the largest percentage in site $A(5)$. This distribution guarantees that no Si–Si contacts occur, except possibly between sites that are occupied by mixtures of Mn and Si. The average percentage of Mn on the sites surrounding a particular site increases with the decrease of the Mn content of that site. The same result was previously obtained for the X phase ($Mn_{45}Co_{40}Si_{15}$; Manor, Shoemaker & Shoemaker, 1972), the ν phase ($Mn_{81\cdot5}Si_{18\cdot5}$; Shoemaker & Shoemaker, 1971) and the K phase ($Mn_{77}Fe_4Si_{19}$; Shoemaker & Shoemaker, 1977).

We wish to thank Dr A. Zalkin of the Lawrence Berkeley Laboratory for making available to us his system of programs on the CDC 7600 computer. We are grateful to the National Science Foundation for financial support.

References

Bardos, D. I. & Beck, P. A. (1965). *Trans. Metall. Soc. AIME*, **233**, 1446–1447.

Cromer, D. T. (1977). *Acta Cryst.* B**33**, 1993–1995.

Cromer, D. T. & Liberman, D. (1970). *J. Chem. Phys.* **53**, 1891–1898.

Iglesias, J. E. & Steinfink, H. (1972). *J. Less-Common Met.* **26**, 45–52.

International Tables for X-ray Crystallography (1962). Vol. III. Birmingham: Kynoch Press.

Komura, Y., Sly, W. B. & Shoemaker, D. P. (1960). *Acta Cryst.* **13**, 575–585.

Kuzma, Yu. B. & Hladyshevskii, E. I. (1964). *Zh. Neorg. Khim.* **9**, 674–681.

Manor, P. C., Shoemaker, C. B. & Shoemaker, D. P. (1972). *Acta Cryst.* B**28**, 1211–1218.

Samson, S. & Gordon, E. K. (1968). *Acta Cryst.* B**24**, 1004–1013.

Shoemaker, C. B. & Shoemaker, D. P. (1963). *Trans. Metall. Soc. AIME*, **230**, 486–490.

Shoemaker, C. B. & Shoemaker, D. P. (1971). *Acta Cryst.* B**27**, 227–235.

Shoemaker, C. B. & Shoemaker, D. P. (1976). *Acta Cryst.* B**32**, 2306–2313.

Shoemaker, C. B. & Shoemaker, D. P. (1977). *Acta Cryst.* B**33**, 743–754.

Smith, G. S., Johnson, Q. & Tharp, A. G. (1967). *Acta Cryst.* **22**, 269–272.